ACES Asian Chemical Editorial Society

doi.org/10.1002/cnma.202200209

CHEMNANOMAT
Research Article

www.chemnanomat.org

Highly Sensitive and Selective Detection of the Antidepressant Amitriptyline Using a Functionalised Graphene-Based Sensor

Ramin Boroujerdi,* Amor Abdelkader, and Richard Paul[a]

Abstract: The accurate measurement of drug concentration in patient samples is vital and is often conducted using point of care devices for therapeutic drug monitoring and other clinical activities. Two dimensional (2D) nanomaterials provide an opportunity to develop miniaturized, affordable and accurate drug sensors, with the promise of developing point of care tests, which are more convenient compared to current techniques that often require advanced instrumentation and laboratory tests. Here we present a reduced graphene oxide-based electrochemical sensor that permits precise measurements of amitriptyline, a well-known anti-depressant. The sensor uses functionalised graphene where amitriptyline selective receptors directly attached to the carbon atoms on the surface of the graphene through diels-alder reaction. The simplicity of the functionalisation procedure along with a tunable receptor used in this study implies that the same method can be used for developing similar selective sensors, simply by changing the small functional groups attached to the receptor molecule. The electrochemical characteristics of the functionalised graphene were studied with cyclic voltammetry, where the sensor demonstrated excellent selectivity, responding only to amitriptyline when tested against closely related tricyclic antidepressants and a range of other psychoactive drugs. The sensor displayed a wider linear range from 1 ng/mL to 80 μg/mL, which covers the concentration range for amitriptyline studied in therapeutic, pharmaceutical, and forensic investigations. The limit of detection of the developed sensor was 1 ng/ml which competes with the detection limit of gas chromatography – mass spectrometry investigated in this study.

Introduction

Tricyclic antidepressants (TCAs) are polycyclic aromatic molecules with a long aliphatic chain attached to the central ring and ended by a secondary or tertiary amine. The middle ring usually contains seven atoms, and in some TCAs, it possesses a nitrogen and forms a heterocyclic ring. TCAs such as amitriptyline, imipramine, protriptyline and trimipramine have been used as medications for treating psychiatric disorders including depression.[1] Amitriptyline (AMT) is a traditional treatment used in clinical practice and its popularity is due to its high clinical effectiveness.[2] AMT has also been used in treatment of Fibromyalgia, an illness characterized by widespread chronic pain, physical exhaustion, cognitive difficulties and depressed mood.[3] Current pharmacotherapy often requires precise dosing of TCAs which can be individual to the patient. Therapeutic drug monitoring is considered by some a useful approach for compounds such as TCAs as these compounds can show variability in blood concentration amongst patients given the same dose.[4] It is therefore important that research continues to develop new technologies that improve the ability of clinicians to monitor drug levels using portable, precise systems. AMT is frequently present in environmental waters that reflects the continuous consumption growth and raises issues on the importance of its monitorization.[5] Measuring the accurate levels of AMT in different samples is not only important for pharmaceutical and clinical purposes, but it is also important for forensic pathologists and toxicologists.[6] AMT is toxic for children and has been implicated in child fatalities.[7] At the same time AMT overdose could cause cardiovascular and neurologic effects such as ventricular arrhythmia, low blood pressure, seizure, and cardiac arrest.[8]

Commonly applied techniques such as gas chromatography,[9] liquid chromatography[10] and high performance liquid chromatography[11] coupled with mass spectrometry, have been applied to detect and measure TCAs, including AMT, in the past decade. There is demand, however, for more affordable and less complicated detection methods which can measure this antidepressant with relatively high sensitivity and selectivity and in a shorter period of time to monitor patients regularly during therapeutic drug monitoring, and also with wider applications in toxicology and forensic investigations.[12] There is also a need for designing portable and at-home tests, that might allow patients to self-monitor and the doctors to regulate the AMT concentrations. This requires a miniaturized, affordable system that can detect AMT selectively, and one that does not suffer from the short lifetime of enzyme or antibody-based biosensors; graphene provides the base to develop an affordable and small device, while chemical functionalisations can survive longer without any need for to be kept at extreme temperatures. Such portable sensors have been introduced before for measuring a range of other analytes such as glucose,[13] SARS-CoV-2,[14] medicines such as levodopa[15] and so

[a] R. Boroujerdi, A. Abdelkader, R. Paul
Faculty of Science and Technology
Bournemouth University
Talbot Campus, Fern Barrow, BH12 5BB Poole (UK)
E-mail: rboroujerdi@bournemouth.ac.uk

forth. However, here we focused on the molecular detection of AMT by developing a highly selective and sensitive electrochemical sensor, which can later be used in commercially available portable potentiostats for on-site testing.[16]

Due to the importance of accurate and precise measurements of AMT for pharmaceutical, medical and forensic studies, other than conventional chromatography based methods,[17] it has been more than three decades since scientists tried to develop a sensitive and selective sensor for measuring amitriptyline.[18] From plastic membrane[18] and molecular imprinted sensors[5] to DNA based biosensors[17c] and using computational modeling,[19] many tried to develop a better amitriptyline sensor in terms of selectivity and sensitivity. Due to the fast response of electrochemical sensors, recent studies tried to utilize cyclic voltammetry and use composites made from conductive materials such as graphite[20] and carbon nano tubes[21] to obtain a fast and reliable sensor. However, previously developed sensors suffer from issues such as being unable to differentiate between different TCAs,[1d] very limited linear range,[17c] or poor detection limit[5,20a] that are not low enough to be used for pharmaceutical studies.[22]

Due to the high surface area, high conductivity and excellent flexibility, which are the some of the most important aspects of two-dimensions (2D) materials, they have been utilized for developing a range of sensors from stationary to portable and wearable sensors. 2D nanomaterials such as graphene, metal oxides, MXenens, transition metal dichalcogenides (TMDs), metal organic frameworks (MOFs), phosphorene are known 2D materials that have attracted the interests in developing electrochemical sensors due to their excellent physical, chemical, and electrical properties. Such 2D nanomaterials have been used to construct high-performance sensors and flexible electronic devices that have potential to revolutionize the conventional detection techniques.[23]

Graphene is a 2D nanomaterial that has attracted a great deal of interest due to its exceptional characteristics that could address the aforementioned challenges, such as high conductivity, high specific surface area, flexibility and mechanical strength.[24] However, graphene by itself cannot interact with the analyte without adding proper chemical functional groups that can interact with the targeted species.[25] To date, graphene has rarely been used for the detection of psychoactive drugs, and its application in developing a selective sensor for AMT has never been reported before.[26] Here we present a novel functionalized reduced graphene oxide-based AMT selective electrochemical sensor for the first time. The sensor is highly selective towards AMT among various tested similar TCAs and other drugs. It can detect AMT in an outstandingly wide linear range and can detect concentrations as low as only 1 ng/mL. The sensor was developed through anchoring functional groups to the carbon atoms on the surface of graphene employing Diels-Alder[27] reaction and forming carbon-carbon bonds between reduced graphene oxide and AMT selective functional group and studied using cyclic voltammetry. The use of the Diels-Alder method here minimized the possibility of developing any side products and let us recycle the unreacted diene for re-use. The diene used in this study has significant potential for further functionalisation[28] and can be tuned to be selective toward other molecules simply by changing its functional groups.

Results and Discussion

Characterizations

ATR-FTIR

The functional groups on GO, rGO, and functionalised graphene were determined using Fourier transform infrared spectroscopy (FTIR) in the range 400 to 4000 cm^{-1}. As can be seen from Figure 1b, the intensity of the wide and strong O–H stretching peak at 3281.80 cm^{-1}[29] detected on the surface of GO significantly decreased after Al reduction process, suggesting successful reduction.[30] The reduction can be further evidenced by the disappearance of the oxide groups peaks at wavelengths below 1500 cm^{-1}. Detecting the C–O stretch at 1054.99 cm^{-1} confirming the successful functionalisation of the rGO through the Diels-Alder reaction.[29b] The spectra of monomer, D1 and D2 is given in Figure 1a; The strong C=O stretching bond which appear at 1673.87 cm^{-1}[31] in the monomer vanished in both D1 and D2, confirming the successful dimerization through the carbonyl site.

Comparing D1 and D2 spectra in Figure 1a, two new peaks can be observed: C–O stretching at 1105.88 cm^{-1} and O–H stretching peak at 3349.11 cm^{-1}. Detecting the O–H peaks confirms the functional group conversion on the diene, from $-OCH_3$ to –OH group. Li et al.[32] suggested that demethylation by BBr_3 will convert both of the methoxy groups to the alcoholic group. However, we noticed that by slight changes in the reaction conditions, the group of peaks between 2800 and 3000 cm^{-1} correspond to the methoxy group ($-OCH_3$)[33] can still be detected. This suggests only one of the methyl groups was replaced by hydrogen and formed –OH and the other one remains unchanged. Sousa and Silva[34] suggested that from two reacted methoxy groups with BBr3, only one methoxy group will convert to an alcoholic group, and the other methoxy group will remain intact; their suggested mechanism was justified via binding energies. In our experiment we see evidence to support this mechanism in the FTIR results of the developed diene (D2). The suggested mechanism of reaction in our experiment is illustrated in Figure 2a.

Raman spectroscopy

The Raman spectra are illustrated in Figure 3. All samples show distinguished G peaks at about 1580 cm^{-1} related to the in-plane vibration of sp^2 hybridized carbon atoms.[35] For GO, rGO and the functionalised samples show D peak at around 1320 cm^{-1}, related to the defects induced during the oxidation of graphite. The ratio I_D/I_G increased after the aluminum reduction, suggesting more defects was introduced in the graphene basal plane during the reduction. Interestingly, the $I_D/$

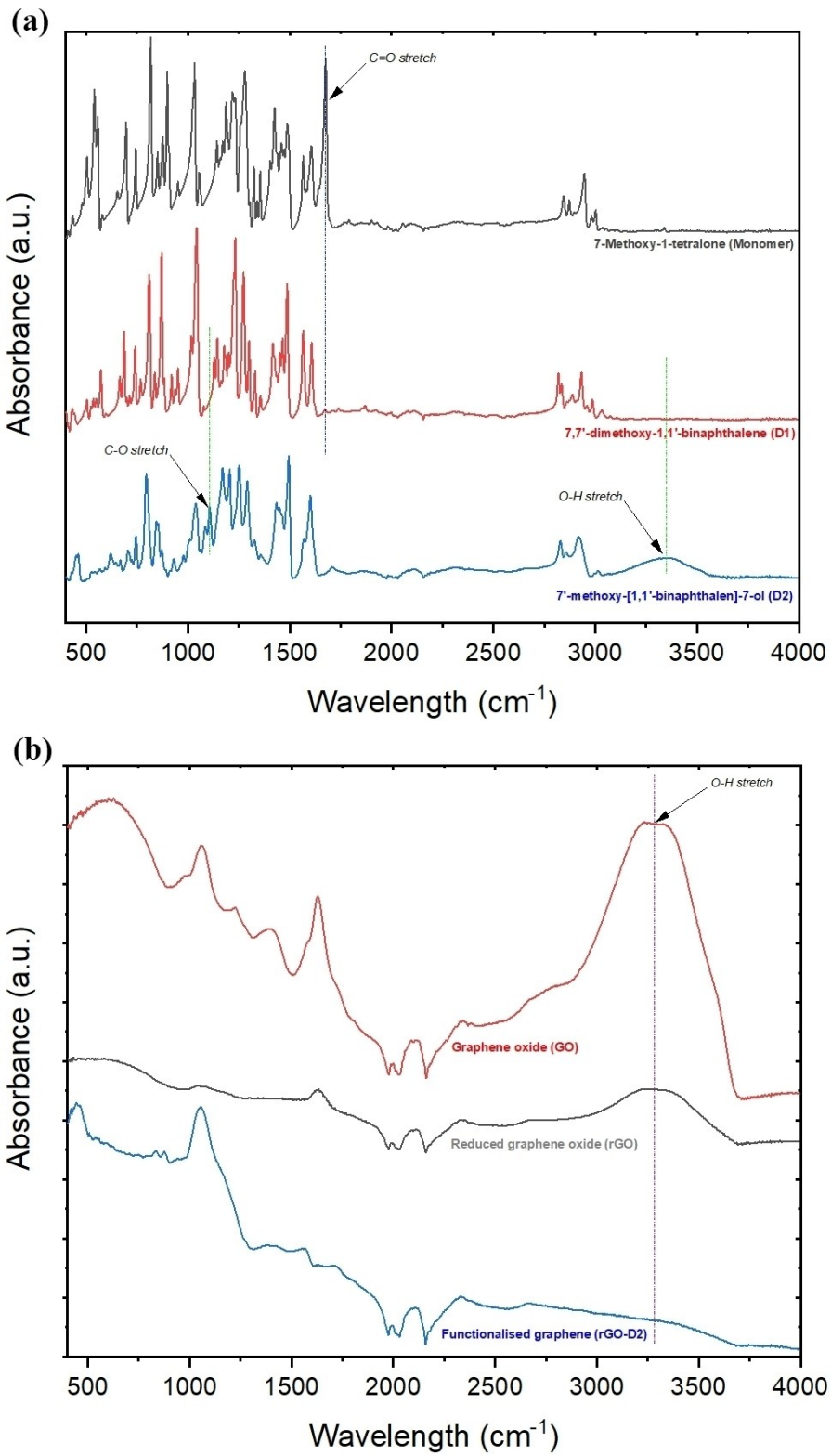

Figure 1. ATR-FTIR spectrums of (a) Monomer, D1 and D2, (b) GO, rGO and rGO-D2.

I_G ratio decreased from 1.79 to 0.87 after the Diels-Alder functionalisation. The decrease in the I_D/I_G ratio is also associated with the appearance of the 2D band at around 2600 cm^{-1}. This is probably due to the interface between the carbon atoms in the graphene plane and the dimerization product (Figure 2b).

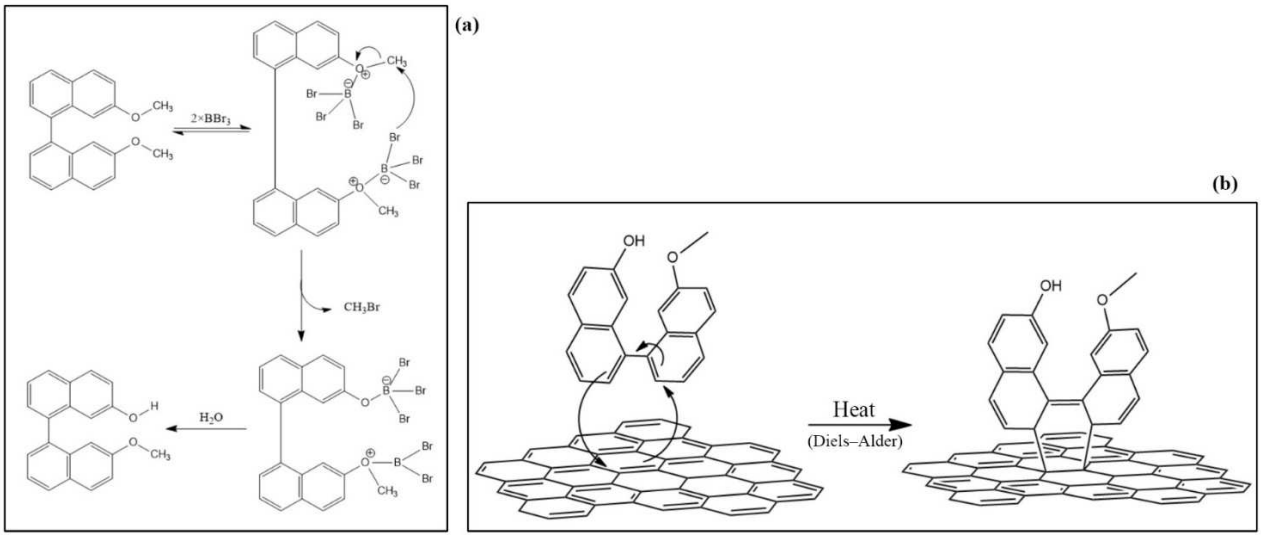

Figure 2. (a) shows the proposed bimolecular pathways for conversion of D1 to D2, while (b) illustrates the functionalisation procedure.

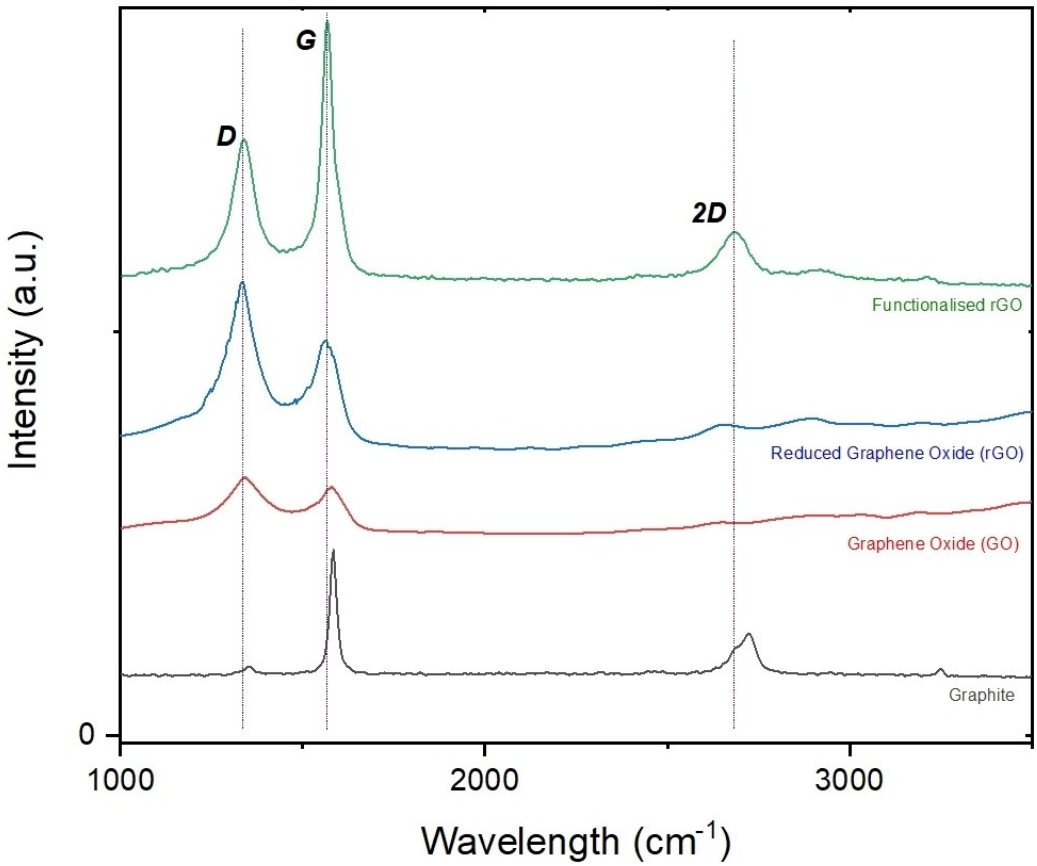

Figure 3. Raman spectra ($\lambda_{exc} = 532$ nm) for graphite, graphene oxide (GO), reduced graphene oxide (rGO) and functionalised rGO.

SEM and EDX analysis

The morphology of the samples was investigated using a scanning electron microscope (SEM) and the impurities were assessed using energy dispersive X-ray analysis (EDX) techniques. The image of the GO samples indicated thin flakes with lateral size in the range 20–50 μm (Figure 4b). These flakes slightly aggregated together after reduction, probably due to the residual charge from the aluminum reducing agent (Figure 4c). The attraction between the localized positive charges

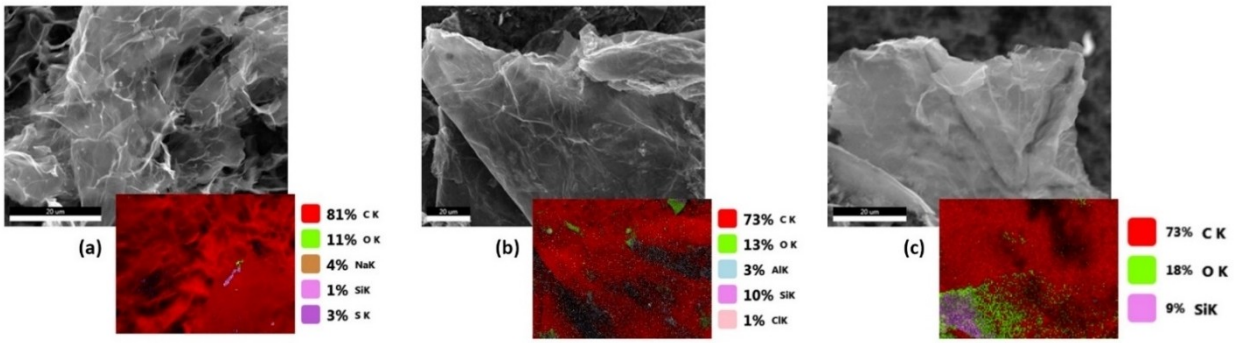

Figure 4. SEM images and EDX graphs for (a) graphene oxide, (b) reduced graphene oxide and (c) functionalised graphene. Scale bars are 20 μm.

caused by aluminum residues and the negatively charged GO flakes might have caused the flakes to aggregate, which is not uncommon for rGO. Not much changes can be observed in the morphology after the Diels-Alder functionalisation. The EDX results of the final functionalised product, despite the presence of SiO_2, shows a slight increase in the percentage of the oxygen (Figure 4d), comparing to the reduced graphene oxide, which could have been caused by attaching diene to the surface of graphene.

Electrochemical behaviors and redox mechanism of amitriptyline on sensor

A comparison of the response of pristine graphene and functionalised graphene to an 80μg/mL amitriptyline solution was conducted to study the effect of functionalisation on the sensitivity of the electrode towards the analyte. As can be seen in Figure 5a, a significant oxidation peak appears only on the graphene electrode functionalised by anchoring diene on its surface, while pristine reduced graphene oxide does not show any sensitivity even towards a high concentration of AMT.

Previous studies on AMT electrooxidation suggested electrode reaction proceeds via oxidation of tertiary amine group at the end of AMT's carbon chain, through a process in which it creates an aminium radical cation.[20b,36] However, previously developed electrodes that suggested such oxidation process had the similar issues in that they could not differentiate between TCAs as almost all of those compounds have the same amine group on their carbon chain. However, considering that among 4 tested TCAs with almost similar amine group (Figure 6), sensor's selective response to AMT (Figure 7a and b) could also be related to AMT's double bond at the beginning of the carbon chain attached to the rings. Since this π-bond forms a stable and slightly larger resonance path, from the rings into the chain, it could be that the 1st or 2nd carbon on the carbon chain, that are in resonance with two nearby cycles, along with the non-bonding electrons have been engaged in the electrochemical reaction in the presence of oxygen functional groups on the diene (i.e. –OH and $–OCH_3$) and therefore generated an oxidation peak to be detected with cyclic voltammetry.[37] It is also worth mentioning that the oxidation peak developed from oxidation of tertiary amine group of AMT showed an oxidation peak at much higher potentials, between 840 and 1340 mV, depending on the solvent, scan rate and reference electrode that they used,[1d,17c,20] while the oxidation peak in this research appears between 140 and 220 mV which can suggest a different oxidation process, other than just amine group, as our sensor can differentiate AMT from other TCAs.

The diffusion coefficient was calculated based on Randles-Sevcik equation[38] as following:

$$I_p = 2.69 \times 10^5 AD^{1/2}n^{3/2}y^{1/2}C$$

The 2.69×10^5 is the constant in the Randles-Sevcik equation, I_p is the peak current (1.156 μA), A is electrode surface area (0.1 cm^2), y is the scan rate (1 mV/s), n, the number of electrons involved, considered to be 1. The concentration (C) of the AMT was 60 μg/mL and the diffusion coefficient (D) of the electrochemical sensor found to be about 3.825×10^{-3} cm^2/s which suggests the slow diffusion on the surface of the electrode, which could have been caused due to the size of the AMT molecule and its specific interaction sites with anchored diene molecules.

In order to study the diffusion effects on the response of the sensor further, the changes in electrical current and oxidation peak potential against a constant concentration of the drug (80 μg/mL) by changes in the scan rate has been monitored (Figure 5b, d and e). Results shows that by increasing the scan rate, the oxidation peak appears at higher potentials while at the same time it generates a slightly more intense current response. The oxidation peak currents at the surface of rGO-D2 electrode in the AMT solution increased linearly with the scan rate in the range from 1 to 25 mV/s, and for scan rates above 25 mV/s, the peak vanishes (Figure 5b). This indicates that the electrode reaction of AMT is a surface confined process. In the scan rates ranging from 1 to 25 mV/s, the liner regression equations are showed in Figure 5e and d, where the linear regression factor (R^2) for changes in peak potential and peak intensity (current) in comparison to scan rates of the sensor found to be 0.98 and 0.99, respectively. Stability and reproducibility of the signal generated by the sensor has been

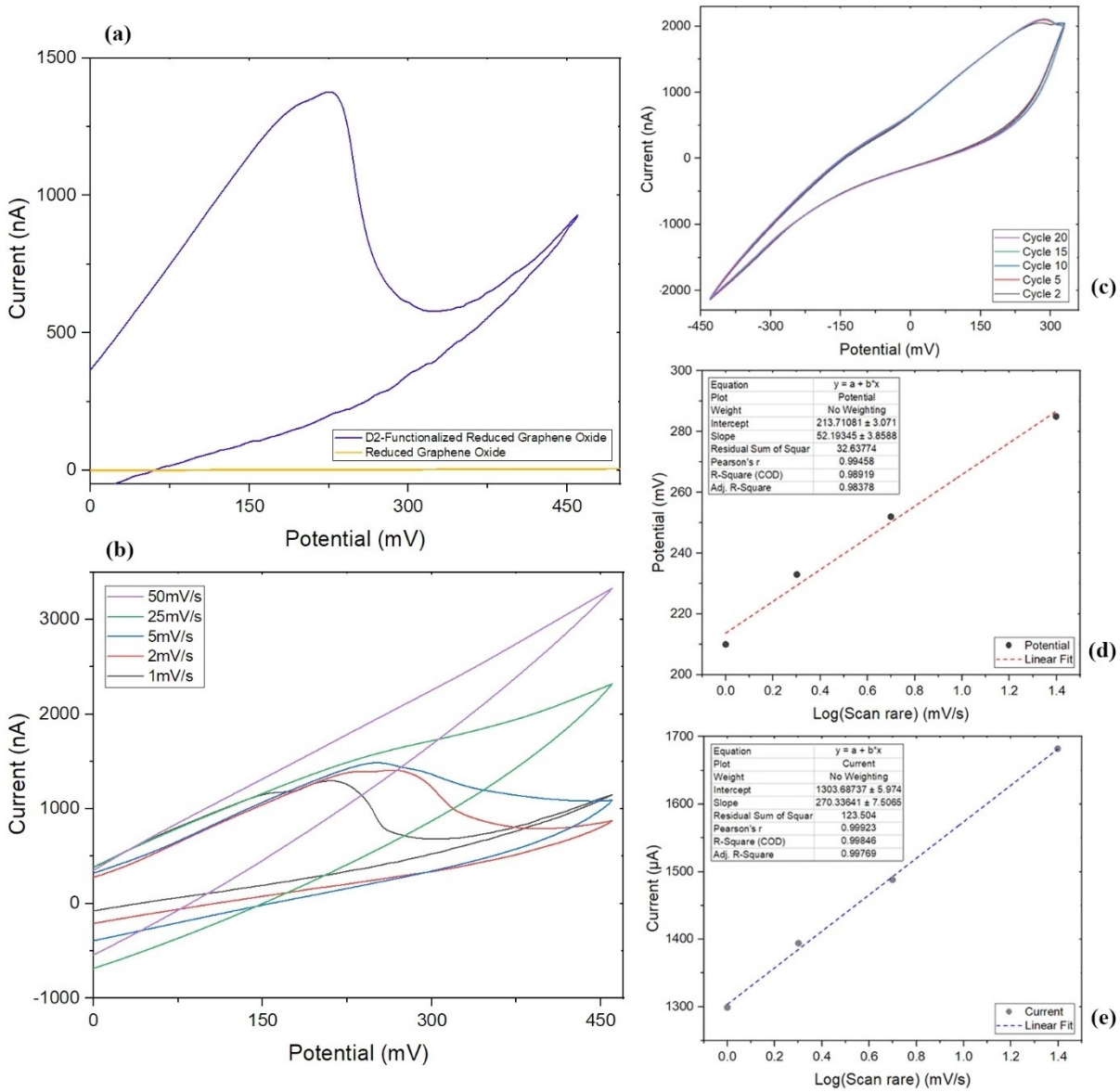

Figure 5. (a) compares the response of reduced graphene oxide before and after adding the D2-functionalisation group to 60µg/mL AMT. (b) shows oxidation peaks obtained from cyclic voltammograms recorded in the presence of 60µg/mL AMT at scan rates of 1, 2, 25 and 50 mV/s at room temperature, while (d) and (e) show the variation of peak potential (mV) and potential intensity (in terms of electrical current; µA) vs the scan rate (mV/s). (c) illustrates the stability and reproducibility of the results by comparing the response of the sensor the same concentration of AMT (80 µg/mL) after 2, 5, 10, 15 and 20 cycles (scan rate: 5 mV/s).

investigated by testing the response of the sensor to the same concentration of AMT over several cycles. The intensity of the oxidation peak at the presence of 80 µg/mL AMT over 20 cycles, where sensors showed reasonable reproducibility of the signal with the RSD of about 1.251% for spectra showed in Figure 5c.

Sensitivity and selectivity of the sensor

The sensitivity of the sensor was investigated by preparing standard solutions of amitriptyline in methanol in the concentration range between 0.5 ng/mL to 100 µg/mL. The response of the functionalised graphene electrode to standard solutions was recorded in the potential window of −0.3 V to +0.46 V using a scan rate of 1 mV/s. The peak current linearly increases with the concentration of the tested drug (Figure 7c and d) in range between the 1 ng/mL to 80 µg/mL. The calculated R^2 value was 0.92 and the lowest concentration that generated a detectable oxidation peak at a signal to noise ratio of at least 3:1 was found to be 1 ng/mL.

The wide linear range suggests that the sensor can be used for analysing a variety of sample types.[39] Medical and pharmaceutical studies on AMT require higher sensitivity as the therapeutic range for amitriptyline is 80–200 ng/mL[22] and its

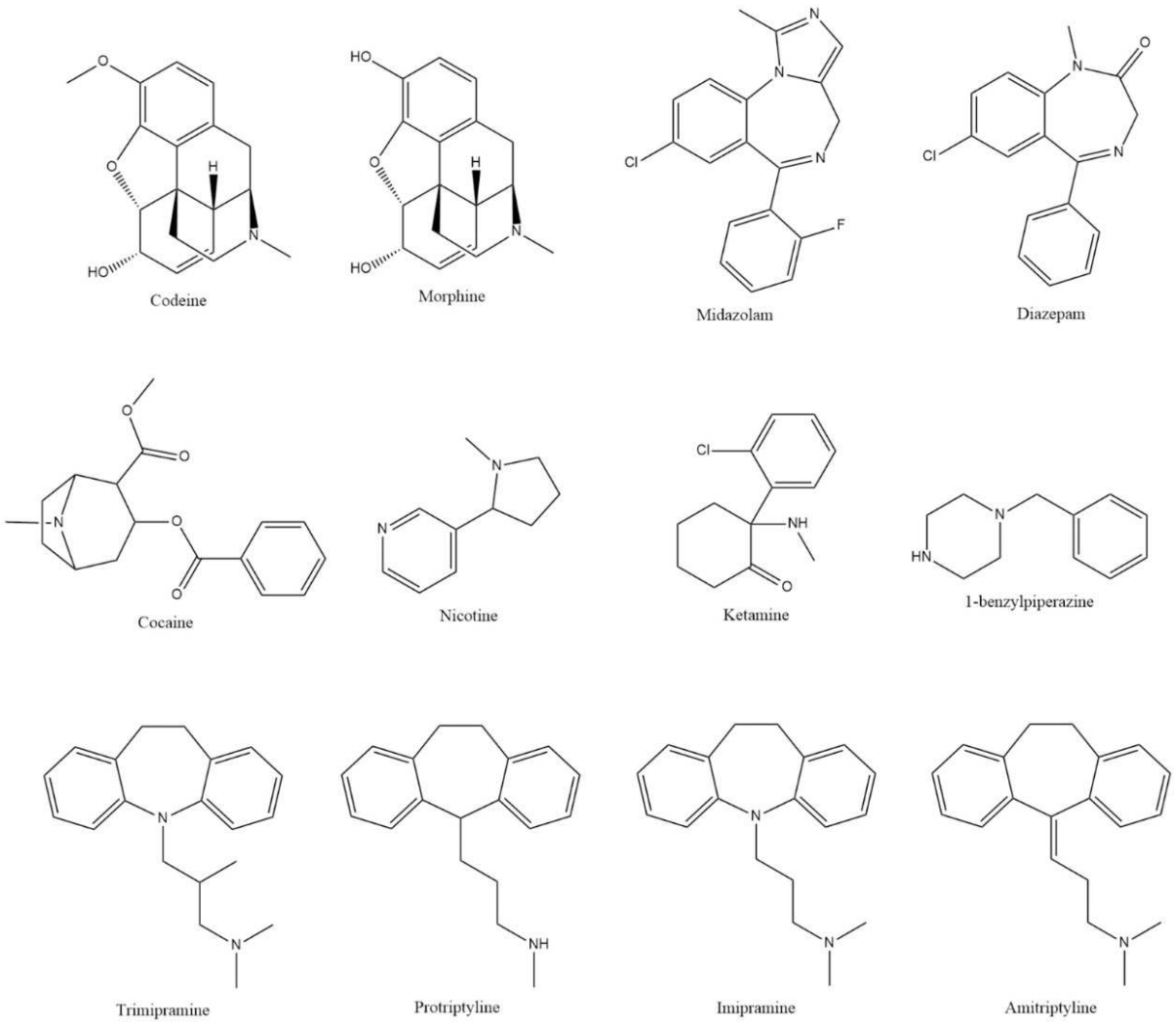

Figure 6. Different drugs used in this study to investigate the selectivity of the sensor.

laboratory alert level is 300 ng/mL.[22] In addition, the sensor can be used for forensic studies as forensic investigations may require a wide concentration range, up to 1.5 μg/mL[40] of AMT, which is also covered by the linear range of the developed sensor.

In order to study the selectivity of the sensor further and investigate its applications as a selective drug sensor, the electrochemical response of the sensor against 12 different drugs (Figure 7) has been tested using cyclic voltammetry. A 0.5 mg/mL standard solution of each of the listed drugs (Figure 7a) in methanol was prepared and the changes in the electrical current in the potential range between −1.0 V to +1.0 V were recorded. The peak current of the oxidation peak at the peak potential compared for all of the 12 drugs. The scan range was intentionally set wider for selectivity tests to confirm the sensor does not generate any other oxidation or reduction peaks in the presence of other tested drugs. The resulting data is illustrated in Figure 7a and b which proved that the sensor is highly selective towards amitriptyline.

A comparative study on amitriptyline detection techniques

The detection of trace level analytes may be performed through selective, direct identification within a complex matrix, or via a separation technique prior to analysis (chromatography for example), based on physical and chemical characteristics. The various approaches may differ in terms of ease of use, affordability and process time, in addition to analytical performance.[26] Here we present the technical evaluation of our AMT sensor compared to an in-house developed GCMS protocol, as well as comparison against a wide range of other detection techniques presented in Table 1. As can be seen in Table 1 the achievement of low detection limits, below 5 ng/ml are usually only obtainable through chromatography-based techniques. Our AMT sensor is the first electrochemical sensor to achieve a detection limit of only 1 ng/ml.

To demonstrate the performance of our sensor we developed a chromatography method for amitriptyline detection using GC-MS. Considered a gold standard for the detection

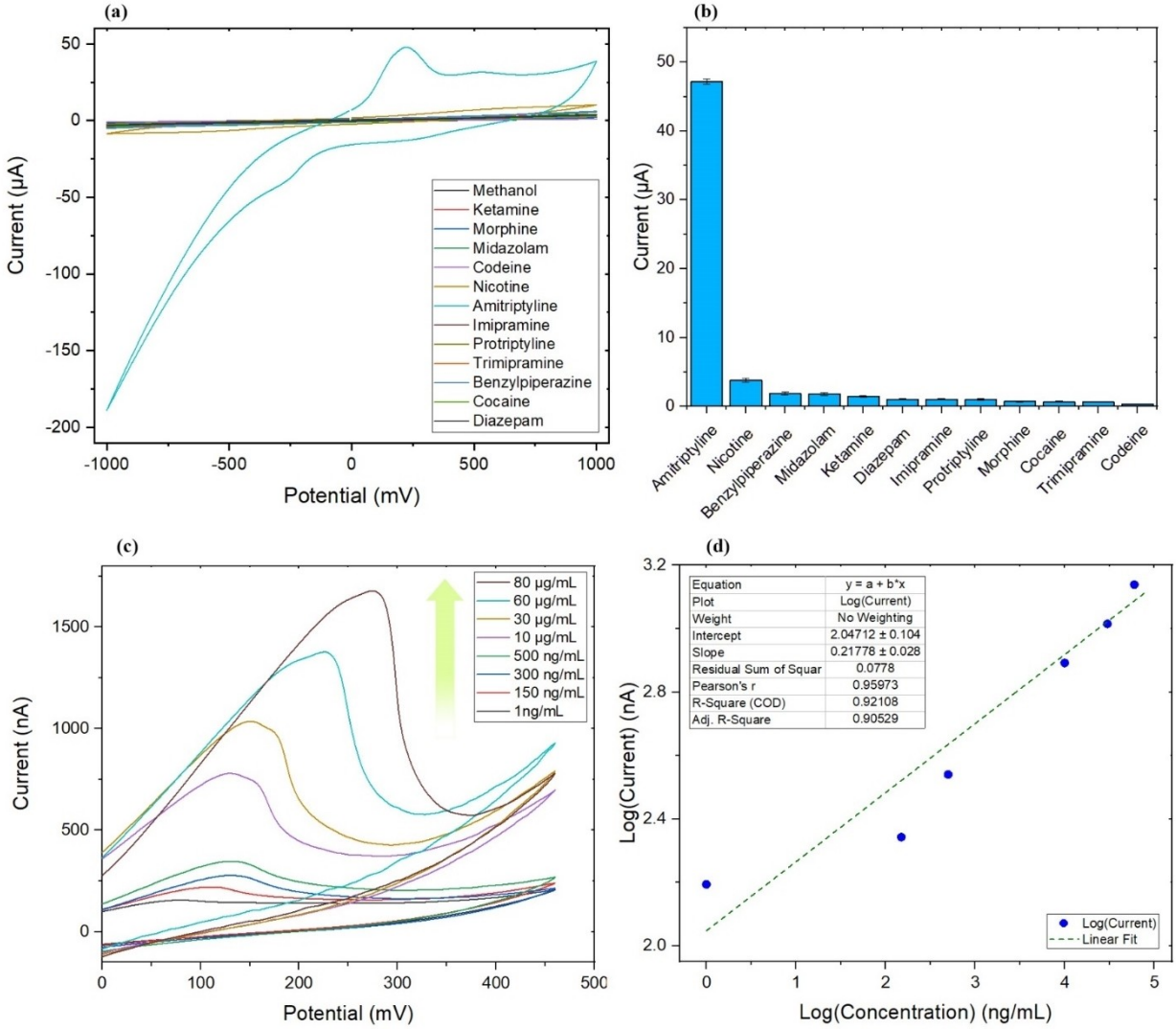

Figure 7. (a) shows the cyclic voltammetry results obtained from testing different drugs, while (b) represents the response of sensor to each drug at the peak potential. (c) displays how the intensity of oxidation peak increases by adding more AMT to the test environment. (d) represents the linear range of the sensor; due to the wide range of the sensor, logarithmic values of concentrations and electrical currents has been used to draw the graph.

Table 1. Comparison of the AMT detection performance of the developed sensor with other techniques.

NO	Detection Technique	Sensing Material	Detection Limit	Ref.
1	Turn-off Fluorescence sensor	Eosin Y	17 ng/mL	[42]
2	Turn-on Fluorescence sensor	Naphthalimide based organic nanoparticles	21 nM	[43]
3	Electrochemiluminescence	Single-walled carbon nanotubes (SWCNT)-molecularly imprinted polymer (MIP)	0.4 μM	[5]
4	Liquid-liquid microextraction – gas chromatography-flame ionization detection (GC-FID)	NA	5 ng/mL	[44]
5	High Pressure Liquid Chromatography – UV detection (HPLC-UV)	Fe_3O_4@ZrO_2@N-cetylpyridinium	0.04 ng/mL	[45]
6	HPLC-UV	NA	4 ng/mL	[46]
7	GC-MS (SIM mode)	NA	2.5 ng/mL	[9c]
8	GC-MS (SIM mode)	NA	0.6 ng/mL	*This work*
9	HPLC-Cyclic voltammetry detection (HPLC-CV)	Highly boron-doped diamond	163 nM	[47]
10	CV	GO-Fe_3O_4@SiO_2	0.5 μM	[48]
11	Linear sweep voltammetry (LSV)	PVC coated glassy carbon (GC) electrode	0.3 nM	[1d]
12	CV	phosphorus-doped multi-walled carbon nanotubes (MWCNT)	150 ng/mL	[49]
13	Differential pulse voltammetry (DPV)	Fe^{3+} exchanged zeolite-clinoptilolite (FeZ) – graphite	220 ng/mL	[50]
14	CV	Reduced graphene oxide – 7′-methoxy-[1,1′-binaphthalen]-7-ol (rGO-D2)	1 ng/mL	*This work*

of such drug compounds, mass spectrometry may serve as a benchmark against which to judge alternative detection techniques. GC-MS analysis of amitriptyline was performed on an Agilent 8890 gas chromatography system coupled to an Agilent 5977B single quadrupole mass selective detector. The column used was a Agilent DB5 ms (30 m × 0.25 mm, 0.25-μL df). The injector and detector temperatures were set to 280 °C. 1 μL standard was used for injection, in splitless mode. The carrier gas used was helium at a flow rate of 1 mL/min. The column temperature was initially set to 60 °C for 2 min, increased to 270 °C at 30 °C/min, and held at 270 °C at 30 °C/min, taking the total run time to 9.7 min. Solvent delay was set to 2 min and electron energy was 70 eV. Full scan data was acquired using EI mode for analysis across the range 50–300 Da. For single ion monitoring (SIM) experiments the amitriptyline fragment ion at 58 Da was monitored (Figure 8a and b). All data was acquired and analyzed using MassHunter software. LOD achieved using full scan mode was 10 ng/mL and LOD achieved in SIM mode was 0.6 ng/mL. Previously reported studies by monitoring m/z 58 for amitriptyline,[41] reported the LOD by GC-MS was found to be between 2.5 ng/mL[9c] and 30 ng/mL,[9b] which matches the results we obtained by testing our standards. Comparing LOD of the GC-MS for amitriptyline with the 1 ng/mL LOD of the developed electrochemical sensor proves that not only is the developed sensor highly selective to AMT amongst other drugs, but it is also highly sensitive to this drug.

Conclusion

In this work a novel modified electrochemical senor, based on functionalised graphene, with a highly selective and sensitive response towards one of the most common antidepressant drugs, amitriptyline was introduced. The wide linear range of the sensor makes it a suitable candidate in a range of applications from medical and pharmaceutical to forensic studies. At the same time its miniaturized design and the application of nanomaterials in its development, make it a viable sensor for on-site testing. The sensor demonstrated exceptional selectivity, only responding to amitriptyline among 12 tested drugs, and it was even able to successfully differentiate between different TCAs with very similar molecular structure and its performance is directly associated with the functionalisation anchored directly to the surface of reduced graphene oxide.

The sensor was fabricated with the help of Diels-Alder reaction which has been used to functionalise the graphene and offers several key benefits such as: simplicity of the reaction

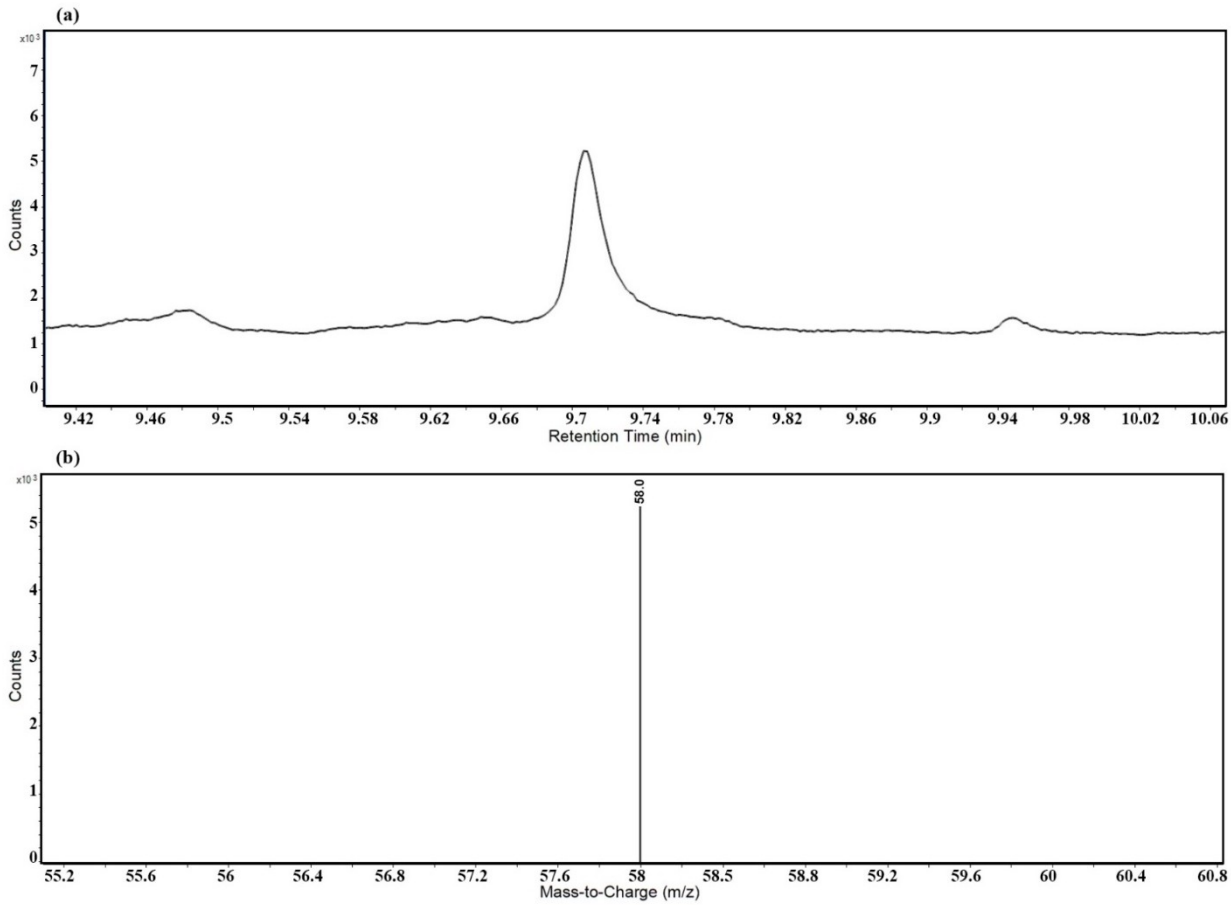

Figure 8. GC-MS analysis of amitriptyline. (a) chromatography at LOD, retention time is 9.7 min (b) Mass spectra in SIM mode, monitoring 58 m/z fragment ion.

procedure, allowing us to recycle and reuse the unreacted diene after filtration of functionalised graphene, minimize the chances of having any other side products and hence offers high purity products. Also, the diene which has been used in this work showed great potential for further functionalisations, which make it a suitable candidate to be used for detecting other drugs after minor modification.

The sensor demonstrated an excellent detection limit for amitriptyline, showing a favourable comparison even with advanced techniques such as GC-MS. When considering the practical benefits of electrochemical sensors including their affordability, and ease of use, this study demonstrates the potential for nanoparticle-based sensors to revolutionize drug detection techniques, particularly where portability is required.

Experimental Section

Reagents and apparatus: All chemicals and reagents including graphite, 7-methoxy-1-tetralone, boron tribromide, mercury (II) chloride, magnesium sulfate, aluminum foil, graphite, potassium permanganate, sodium nitrate, hydrogen peroxide and solvents including toluene, ethanol, methanol and acids were purchased from Fisher Scientific, UK, and were of analytical reagent grade. All chemicals were used without prior purifications. RVFM A3 thin copper sheets (0.1 mm thickness) were used as the substrate. Aqueous solutions were prepared using purified distilled water.

Cyclic voltammetry and electrochemical measurements were conducted at room temperature using IviumStat.h (Ivium Technologies, Netherlands) potentiostat. The measuring cell was in a three-electrode configuration with 1.5 mL volume. The developed graphene-based sensors were used as the working electrode, Ag/AgCl as the reference electrode and Pt as the counter electrode. Graphene-based ink was made in an ultrasonic bath (U500H UI, Ultrawave, UK) and printed electrodes on the previously made patterns were dried in a vacuum oven (Jeio Tech's OV-11, South Korea). Platinum ATR – Alpha II FTIR spectrophotometer (Bruker, USA) was applied to collect Fourier transform infrared (FTIR) spectra. XploRA™ PLUS Raman spectrometer was used to collect Raman spectra. JEOL JSM-6010 tungsten cathode scanning electron microscope was used to carry out both scanning electron microscopy-energy dispersive spectroscopy (SEM and EDX) analysis.

Preparation of graphene oxide and reduced graphene oxide: Graphene oxide was produced by the modified Hummers[51] methods using natural graphite as the raw materials. To produce reduced graphene oxide (rGO), we have used aluminum as a reducing agent in hydrochloric acid, as outlined elsewhere.

Preparing of functional groups: In this study, while graphene is going to act as a dienophile[32,52], the chosen functional group is going to be a large organic molecule which has selective receptors on one end and with two adjacent (i.e. conjugated) pi bonds on its other end, which will act as a diene, which allows formation of direct C–C bonds between functional group and carbon atoms on reduced graphene oxide through Diels-Alder reaction.

7,7′-dimethoxy-1,1′-binaphthalene (D1)

The main structure of the functional groups for modification and functionalisation of graphene layers, is an aromatic molecule made of four carbon rings: 7,7′-dimethoxy-1,1′-binaphthalene (D1), which was developed through a slightly modified version of Li's method.[32] D1 is a diene made by dimerization of its monomer, 7-methoxy-1-tetralone. The dimerization process starts when 10 grams of 7-methoxy-1-tetralone and 0.1 grams of $HgCl_2$ a mixture of toluene (50 mL) and ethanol (30 mL) was combined. To the transparent outcome solution 1.6 grams aluminum foil (cut into small pieces) was added and the solution is kept under vigorous stirring. The foil was added to the solution slowly and the color of the solution changed to gray. After 6 hours the reflux heating was stopped but vigorous stirring continued and 50 mL diluted HCl (10%) was added to the flask through the condenser in two 25 mL portions which leads to changing the color of the solution to white. The solution kept under stirring for another 2 hours and the color of the solution turn to yellow and all the aluminum dissolves. The organic phase of solution separated and placed in a closed chamber over $MgSO_4$ for 12 hours to remove the water. The transparent orange solution was dried under vacuum conditions at 30 °C to form dark orange crystals. Dried product then transferred to the reflux flask and dissolved in a mixture of acetic anhydride (60 mL) and acetic acid (40 mL) and refluxed started. After 6 hours reflux the stirring stopped and the solution left to cool down slowly. Yellow crystals of diene will form in the outcome brown solution as soon as the solution is shaken. The solution was filtered three times and outcome solids washed with a mixture of acetic anhydride and acetic acid and dried under the safety hood (Figure 9).

7′-methoxy-[1,1′-binaphthalen]-7-ol (D2)

The second diene (D2) was obtained from demethylation of D1. Firstly, 4 grams of D1 were completely dissolved in 15 mL dichloromethane. Afterwards, the solution was transferred to −78 °C dry-ice/acetone bath while stirring and 2 mL BBr_3 drop by drop was added to react with methoxy groups. After 3 hours stirring, 2 grams of pure 0 °C ice (H_2O) added to the mixture to react and turn –O–CH_3 groups of the D1 into –O–H and finalize demethylation. After 1 hour, the organic phase was then separated, washed with

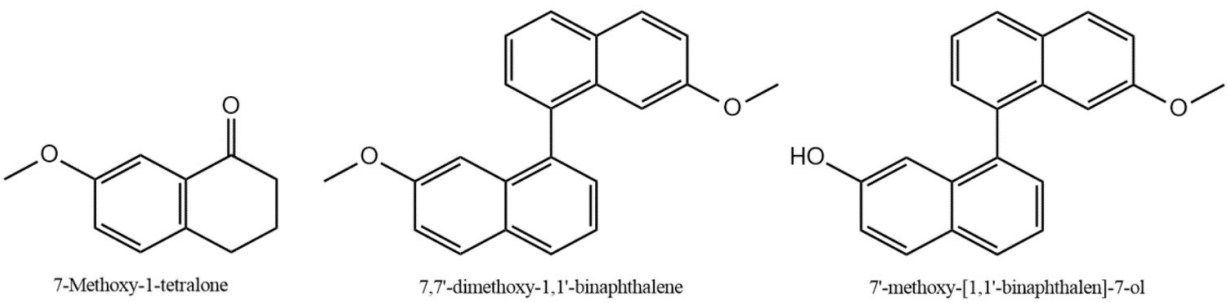

Figure 9. Monomer molecule compared to synthesised dienes, D1 and D2, from left to right, respectively.

pure water (mix, shake and separation of organic phase again) and finally dried under the fume hood.

Functionalisation procedure: Diels-Alder reaction was used to attach the developed dienes to rGO. Li et al reported that the drop-heating method and reflux may both allow Diels-Alder reaction to occur between graphene/SiO_2 and diene.[32] Here we used the reflux method with some modifications. The Dienes dissolved in dichloroethane, while rGO was ultrasonically dispersed in the same solvent in a separate container. Both solutions were then mixed together and slowly stirred while refluxed at about 120 °C for 5 hours.

Electrode fabrication: Functionalised graphene samples were sonicated in dimethylformamide and then mixed with polyethylene terephthalate (PET; 10 wt% of graphene) using mild sonication. The electrode was then prepared using the doctor blade method on copper foil and heated under vacuum up to 130 °C for 24 h to remove all the residual solvents.

Acknowledgements

The authors thank Surescreen Diagnostics Ltd for funding this work (Ref: 10757).

Conflict of Interest

The authors declare no conflict of interest.

Data Availability Statement

The data that support the findings of this study are available from the corresponding author upon reasonable request.

Keywords: amitriptyline sensor · graphene · pharmaceutical analysis · printable electrodes · toxicology

[1] a) N. Manousi, V. F. J. S. Samanidou, *Separations* **2019**, *6*, 24; b) V. Samanidou, M. Nika, I. Papadoyannis, *Mini Rev. Med. Chem.* **2008**, *8*, 256; c) F. Mofazzeli, H. Asaadi Shirvan, F. J. Mohammadi, *J. Sep. Sci.* **2018**, *41*, 4340; d) M. Guzinski, E. Lindner, B. Pendley, E. Chaum, *Talanta* **2022**, *239*, 123072; e) Y. Subasi, G. S. Kanberoglu, F. Coldur, O. Cubuk, M. Zahmakiran, *Chem. Pap.* **2022**, *1*; f) E. Medyantseva, E. Gazizullina, D. Brusnitsyn, M. Ziganshin, Y. G. Elistratova, A. Mustafina, K. Brylev, H. J. Budnikov, *J. Anal. Chem.* **2021**, *76*, 1455.

[2] a) Y. Jie, D. Shuang, Z. Xinjie, *Trop. J. Pharm. Res.* **2019**, *18*, 403; b) V. Melin, P. Salgado, A. Thiam, A. Henríquez, H. D. Mansilla, J. Yáñez, C. Salazar, *Chemosphere* **2021**, *274*, 129683.

[3] H. M. Farag, I. Yunusa, H. Goswami, I. Sultan, J. A. Doucette, T. Eguale, *JAMA Netw. Open* **2022**, *5*, e2212939.

[4] L. F. Gram, *Clin. Pharmacokinet.* **1977**, *2*, 237.

[5] P. Rebelo, J. G. Pacheco, I. V. Voroshylova, M. N. D. Cordeiro, C. Delerue-Matos, *Electrochim. Acta* **2021**, *397*, 139273.

[6] J. A. Prahlow, J. E. Landrum, pathology, *Am. J. Forensic Med. Pathol.* **2005**, *26*, 86.

[7] a) H. Çaksen, S. Akbayram, D. Odabaş, H. Özbek, M. Erol, C. Akgün, O. Tuncer, C. Yilmaz, e. toxicology, *Hum. Exp. Toxicol.* **2006**, *25*, 107; b) K. Goel, R. A. Shanks, *Br. Med. J.* **1974**, *1*, 261.

[8] a) P. T. Engels, J. S. Davidow, *Resuscitation* **2010**, *81*, 1037; b) M. Levine, D. E. Brooks, A. Franken, R. Graham, *Pediatrics* **2012**, *130*, e432; c) B.-Å. Hultén, A. Heath, K. Knudsen, G. Nyberg, J.-E. Starmark, E. J. Mårtensson, *Clin. Toxicol.* **1992**, *30*, 171.

[9] a) J. Lee, J. Park, A. Go, H. Moon, S. Kim, S. Jung, W. Jeong, H. Chung, *J. Anal. Toxicol.* **2018**, *42*, 617; b) L. Truta, A. L. Castro, S. Tarelho, P. Costa, M. G. F. Sales, H. M. Teixeira, *J. Pharmac. Biomed. Anal.* **2016**, *128*, 496; c) T. Rosado, A. Gonçalves, A. Martinho, G. Alves, A. P. Duarte, F. Domingues, S. Silvestre, L. B. Granadeiro, V. Oliveira, C. Leitão, E. Gallardo, *Chromatographia* **2017**, *80*, 301; d) E. Ferrari Júnior, E. D. Caldas, *Forensic Sci. Int.* **2018**, *290*, 318; e) S. Tetteh, A. Monney, R. Zugle, J. K. Adjei, *Front. Chem. Res.* **2019**, *1*, 31.

[10] a) L. Mifsud Buhagiar, C. Sammut, Y. Chircop, K. Axisa, N. Sammut Bartolo, J. Vella Szijj, A. Serracino Inglott, G. LaFerla, *Biomed. Chromatogr.* **2019**, *33*, e4679; b) A. T. Caspar, M. R. Meyer, H. H. Maurer, *Drug Test. Anal.* **2019**, *11*, 102; c) E. N. Ediage, T. Aerts, A. Lubin, F. Cuyckens, L. Dillen, T. Verhaeghe, *Bioanalysis* **2019**, *11*, 1189; d) A. Lubin, R. De Vries, D. Cabooter, P. Augustijns, F. Cuyckens, *J. Pharmac. Biomed. Anal.* **2017**, *142*, 225; e) I. Kasagić-Vujanović, B. J. Jančić-Stojanović, B. Analysis, *J. Pharm. Biomed.* **2019**, *173*, 86.

[11] a) A. Muni Krishnaiah, C. Rama Chandraiah, M. Srinivas, N. Devanna, *Rasayan J. Chem.* **2020**, *13*, 24; b) A. Lioupi, A. Kabir, K. G. Furton, V. Samanidou, *J. Chromatogr. B* **2019**, *1118–1119*, 171; c) S. Shaikh, V. Jain, *Int. J. Appl. Pharmac.* **2018**, *10*, 97; d) J. L. Poklis, C. E. Wolf, A. Goldstein, M. L. Wolfe, A. Poklis, *J. Clin. Lab. Anal.* **2012**, *26*, 286; e) A. J. Vyas, G. P. Nathwani, A. I. Patel, N. K. Patel, A. B. Patel, *Chem. Methodol.* **2019**, *3*, 494.

[12] A. Saini, R. Kaur, N. Singh, A. Kuwar, N. Kaur, *ACS Appl. Bio Mater.* **2018**, *2*, 135.

[13] C. Zhang, Z. Zhang, Q. Yang, W. Chen, *Electroanalysis* **2018**, *30*, 2504.

[14] a) D. K. Ban, T. Bodily, A. G. Karkisaval, Y. Dong, S. Natani, A. Ramanathan, A. Ramil, S. Srivastava, P. Bandaru, G. Glinsky, *PNAS* **2022**, *119*, e2206521119; b) R. M. Torrente-Rodríguez, H. Lukas, J. Tu, J. Min, Y. Yang, C. Xu, H. B. Rossiter, W. Gao, *Matter* **2020**, *3*, 1981.

[15] J. Xiao, C. Fan, T. Xu, L. Su, X. Zhang, *Sens. Actuators B* **2022**, *359*, 131586.

[16] a) P. Pansodtee, J. Selberg, M. Jia, M. Jafari, H. Dechiraju, T. Thomsen, M. Gomez, M. Rolandi, M. Teodorescu, *Plos one* **2021**, *16*, e0257167; b) S. Nagabooshanam, S. Roy, A. Mathur, I. Mukherjee, S. Krishnamurthy, L. M. Bharadwaj, *Sci. Rep.* **2019**, *9*, 19862; c) S. D. Adams, E. H. Doeven, K. Quayle, A. Z. Kouzani, *Ieee Access* **2019**, *7*, 31903; d) M. Rahman, A. Raihan, D. A. Muhtasim, S. Farhana, O. Faruk, *J. IJRPR 2582*, 7421; e) A. Scott, S. Sakib, S. Saha, I. Zhitomirsky, L. Soleymani, *Electrochim. Acta* **2022**, *419*, 140347.

[17] a) C. K. Markopoulou, E. T. Malliou, J. E. J. J. o. p. Koundourellis, b. analysis, *J. Pharm. Biomed.* **2005**, *37*, 249; b) M. R. Jalali Sarvestani, R. Ahmadi, *J. Phys. Theor. Chem.* **2018**, *15*, 15; c) J. P. Marco, K. B. Borges, C. R. T. Tarley, E. S. Ribeiro, A. C. Pereira, *J. Electroanal. Chem.* **2013**, *704*, 159.

[18] A. A. Bunaciu, M. S. Ionescu, C. Pălivan, V. V. Coşofreţ, *Analyst* **1991**, *116*, 239.

[19] M. R. Jalali Sarvestani, Z. Doroudi, *J. Chem. Lett.* **2020**, *1*, 63.

[20] a) H. Beitollai, F. Garkani Nejad, S. Tajik, S. Jahani, P. Biparva, *Int. J. Nano Dimens.* **2017**, *8*, 197; b) M. Madej, K. Fendrych, R. Porada, M. Flacha, J. Kochana, B. Baś, *Microchem. J.* **2021**, *160*, 105648.

[21] A. A. P. Khan, *Materials* **2020**, *13*, 1708.

[22] C. Hiemke, P. Baumann, N. Bergemann, A. Conca, O. Dietmaier, K. Egberts, M. Fric, M. Gerlach, C. Greiner, G. Gründer, *Pharmacopsychiatry* **2011**, *21*, 195.

[23] a) D. Zhang, Z. Xu, Z. Yang, X. Song, *Nano Energy* **2020**, *67*, 104251; b) D. Zhang, M. Wang, W. Zhang, Q. Li, *Sens. Actuators B* **2020**, *304*, 127234; c) D. Zhang, D. Wang, P. Li, X. Zhou, X. Zong, G. Dong, *Sens. Actuators B* **2018**, *255*, 1869; d) D. Wang, D. Zhang, P. Li, Z. Yang, Q. Mi, L. Yu, *Nano-Micro Lett.* **2021**, *13*, 57; e) D. Wang, D. Zhang, M. Tang, H. Zhang, F. Chen, T. Wang, Z. Li, P. Zhao, *Chem. Eng. J.* **2022**, *446*, 136914; f) D. Wang, D. Zhang, Y. Yang, Q. Mi, J. Zhang, L. Yu, *ACS Nano* **2021**, *15*, 2911.

[24] a) R. Boroujerdi, A. Abdelkader, R. Paul, *Nano-Micro Lett.* **2020**, *12*, 33; b) Z. Chen, J. Wang, Y. Wang, *Talanta* **2021**, *235*, 122745; c) R. Boroujerdi, R. Paul, *Chemosensors* **2022**, *10*, 42; d) R. Boroujerdi, A. Abdelkader, R. Paul, *Sens. Diagn.* **2022** *1*, 566-578.

[25] V. Georgakilas, M. Otyepka, A. B. Bourlinos, V. Chandra, N. Kim, K. C. Kemp, P. Hobza, R. Zboril, K. S. Kim, *Chem. Rev.* **2012**, *112*, 6156.

[26] R. Boroujerdi, R. Paul, *Nanomaterials* **2022**, *12*, 2250.

[27] F. Fringuelli, A. Taticchi, in *The Diels-Alder reaction: selected practical methods*, John Wiley & Sons, **2002**.

[28] J. D. Chen, H. Y. Lu, C. F. Chen, *Chem.–A Eur. J.* **2010**, *16*, 11843.

[29] a) E. Ghiamati, R. Boroujerdi, *J. Fluorescence* **2016**, *26*, 135; b) P. Larkin, in *Infrared and Raman spectroscopy: principles and spectral interpretation*, Elsevier, **2017**.
[30] A. M. Abdelkader, *J. Mater. Chem. A* **2015**, *3*, 8519.
[31] C. Yohannan Panicker, H. Tresa Varghese, D. Philip, *Spectrochim. Acta Part A* **2006**, *65*, 802.
[32] J. Li, M. Li, L.-L. Zhou, S.-Y. Lang, H.-Y. Lu, D. Wang, C.-F. Chen, L.-J. Wan, *J. Am. Chem. Soc.* **2016**, *138*, 7448.
[33] J. S. Huberty, R. J. Madix, *Surf. Sci.* **1996**, *360*, 144.
[34] C. S. Silva, P. J. Silva, *Eur. J. Org. Chem.* **2013**, *1*.
[35] a) R. Kumar, B. R. Mehta, M. Bhatnagar, S. Ravi, S. Mahapatra, S. Salkalachen, P. Jhawar, *Nanoscale Res. Lett.* **2014**, *9*, 1; b) Z. Ni, Y. Wang, T. Yu, Z. Shen, *Nano Res.* **2008**, *1*, 273.
[36] a) E. H. Duarte, W. P. dos Santos, F. F. Hudari, J. L. B. Neto, E. R. Sartori, L. H. Dall, A. C. Pereira, C. R. T. Tarley, *Talanta* **2014**, *127*, 26; b) Z. R. Zad, S. S. H. Davarani, A. R. Taheri, Y. J. B. Bide, *Bioelectronics* **2016**, *86*, 616.
[37] a) M. Peover, B. J. J. o. E. C. White, *Electrochemistry* **1967**, *13*, 93; b) X. Hu, G. Zhang, L. Nie, T. Kong, A. Lei, *Nat. Commun.* **2019**, *10*, 1.
[38] a) M. Bogdan, D. Brugger, W. Rosenstiel, B. Speiser, *J. Cheminform.* **2014**, *6*, 1; b) K. Ahmad, P. Kumar, S. M. Mobin, *Nanoscale Adv.* **2020**, *2*, 502; c) D. J. MacArthur, *J. Electrochem. Soc.* **1970**, *117*, 729.
[39] A. Asghari, Z. Saffarzadeh, M. Bazregar, M. Rajabi, L. Boutorabi, *Microchem. J.* **2017**, *130*, 122.
[40] R. A. Ketola, P. J. D. t. Kriikku, *Analysis* **2019**, *11*, 1338.
[41] D. W. Sadler, J. Richardson, S. Haigh, G. Bruce, D. J. Pounder, *Am. J. Forensic Med. Pathol.* **1997**, *18*, 397.
[42] K. Kaur, A. K. Malik, *J. Fluorescence* **2013**, *23*, 533.
[43] A. Saini, R. Kaur, N. Singh, A. Kuwar, N. Kaur, *ACS Appl. Bio Mater.* **2019**, *2*, 135.
[44] A. S. Yazdi, N. Razavi, S. R. Yazdinejad, *Talanta* **2008**, *75*, 1293.
[45] F. Zare, M. Ghaedi, A. Daneshfar, *Microchim. Acta* **2015**, *182*, 1893.
[46] M. T. Hamed Mosavian, Z. Es'haghi, N. Razavi, S. Banihashemi, *J. Pharmac. Anal.* **2012**, *2*, 361.
[47] T. A. Ivandini, B. V. Sarada, C. Terashima, T. N. Rao, D. A. Tryk, H. Ishiguro, Y. Kubota, A. Fujishima, *J. Electroanal. Chem.* **2002**, *521*, 117.
[48] N. Zoheira Bagheri, N. Fariba Garkani, *Surf. Eng. Appl. Electrochem.* **2022**, *58*, 100.
[49] C. Sanguarnsak, K. Promsuwan, J. Saichanapan, A. Soleh, K. Saisahas, C. H. Phua, W. Limbut, *J. Electrochem. Soc.* **2022**, *169*, 017510.
[50] M. Madej, K. Fendrych, R. Porada, M. Flacha, J. Kochana, B. Baś, *Microchem. J.* **2021**, *160*, 105648.
[51] W. S. Hummers, Jr., R. E. Offeman, *J. Am. Chem. Soc.* **1958**, *80*, 1339.
[52] a) Y. Cao, S. Osuna, Y. Liang, R. C. Haddon, K. Houk, *J. Am. Chem. Soc.* **2013**, *135*, 17643; b) S. Sarkar, E. Bekyarova, S. Niyogi, R. C. Haddon, *J. Am. Chem. Soc.* **2011**, *133*, 3324; c) P. A. Denis, *Chem.–A Eur. J.* **2013**, *19*, 15719.

Manuscript received: May 5, 2022
Revised manuscript received: July 19, 2022
Accepted manuscript online: July 22, 2022
Version of record online: August 4, 2022